

DNA hyper-methylation associated with schizophrenia may lead to breakdown of self-tolerance

Hui Wei

State Key Laboratory of Medical Molecular Biology, Institute of Basic Medical Sciences Chinese Academy of Medical Sciences, School of Basic Medicine Peking Union Medical College

Yanbo Yuan

Peking University Sixth Hospital, Peking University Institute of Mental Health, NHC Key Laboratory of Mental Health (Peking University), National Clinical Research Center for Mental Disorders (Peking)

Caiyun Zhu

State Key Laboratory of Medical Molecular Biology, Institute of Basic Medical Sciences Chinese Academy of Medical Sciences, School of Basic Medicine Peking Union Medical College

Mingjie Ma

State Key Laboratory of Medical Molecular Biology, Institute of Basic Medical Sciences Chinese Academy of Medical Sciences, School of Basic Medicine Peking Union Medical College

Fude Yang

Beijing HuiLongGuan Hospital, Beijing

Zheng Lu

Shanghai Mental Health Center

Chuanyue Wang

Beijing Anding Hospital

Hong Deng

Mental Health Center, West China Hospital, Sichuan University

Jingping Zhao

Central South University

Runhui Tian

Mental Health Center, the First Bethune Hospital of Jilin University

Wanwan Zhu

State Key Laboratory of Medical Molecular Biology, Institute of Basic Medical Sciences Chinese Academy of Medical Sciences, School of Basic Medicine Peking Union Medical College

Yan Shen

Institute of Basic Medical Sciences Chinese Academy of Medical Sciences

Xin Yu

Peking University Sixth Hospital <https://orcid.org/0000-0003-3983-4937>

Qi Xu (✉ qixu@vip.sina.com)

State Key Laboratory of Medical Molecular Biology, Institute of Basic Medical Sciences Chinese Academy of Medical Sciences, School of Basic Medicine Peking Union Medical College

Article

Keywords: Biomarkers, Environmental Stressors, Autoimmune Responses, cg14341177 Methylation, Anti-BICD2 IgG, PANSS Scores

Posted Date: July 12th, 2021

DOI: <https://doi.org/10.21203/rs.3.rs-645110/v1>

License:  This work is licensed under a Creative Commons Attribution 4.0 International License. [Read Full License](#)

Abstract

Environmental stressors have effects on the genomic DNA methylation patterns of B lymphocytes in schizophrenia (SCZ), which may therefore perturb the immune homeostasis and trigger autoimmune responses. This study aimed to investigate the global genomic DNA methylation differences in remitters of SCZ (RSCZ) and non-remitters of SCZ (NRSCZ), further their effects on autoimmune responses of target genes. A total of 2722 Chinese Han origin subjects were recruited, including a follow-up cohort and a cross-sectional cohort. We found a DMS of cg14341177 in SCZ which inhibit the mRNA alternative splicing of *BICD2*, further leading to increased plasma anti-BICD2 IgG autoantibody levels. The levels of cg14341177 methylation and anti-BICD2 IgG decreased significantly in the endpoint samples of RSCZ, but not in NRSCZ. There are strong positive correlations between cg14341177 methylation, anti-BICD2 IgG, and PANSS scores. These data suggest that cg14341177 methylation and anti-BICD2 IgG levels may potentially serve as useful biomarkers.

Introduction

Schizophrenia (SCZ) is a severe debilitating disorder, affecting 0.7% of the population worldwide¹. The etiology of SCZ is complicated, wherein both genetic and environmental factors play important roles in its development, leading to high heterogeneity in patient populations.

Recent studies have highlighted a neuro-immune mechanism in the pathogenesis of SCZ, especially with regard to the chronic neuro-inflammatory responses. The literatures on the genome-wide association study (GWAS) in the last five years confirmed hundreds of genetic loci that are significantly associated with the risk of SCZ^{2,3}. The most remarkable genetic association signal is the human leukocyte antigen (HLA) region in the short arm of chromosome 6, which exhibits an autoimmune role in SCZ². The spatiotemporal expression of SCZ-GWAS candidate genes is highly associated with the key time point in neurodevelopment processes. Certain genes are highly expressed in brain tissues and B lymphocytes, which further support the psycho-neuro-immunological hypothesis in SCZ^{2,3}. A study pertaining to SCZ-GWAS candidate genes reported altered autoantibody levels in first-episode schizophrenia (FES) patients⁴. SCZ-GWAS gene-derived autoantigen treatments in cultured B lymphocytes enhance the proportions of CD83+ cells and apoptotic B cells, which suggests a tolerance breakdown mechanism in SCZ⁵.

However, the heterogeneous spectrum of SCZ and divergent responses to antipsychotic medications cannot be solely explained through genetics, but also requires environmental factors to be taken into consideration⁶. Epigenetics can better explain the gene-environment interactions for the disease^{7,8}. The different responses to antipsychotic treatment in patients with SCZ are assumed because of DNA methylation and histone modification patterns^{7,9}. Several studies that focused on differential DNA methylation patterns in SCZ^{9,10,11,12,13}, and have identified differentially regulated DNA methylation biomarkers involved in divergent antipsychotic medication responses⁷. In rodent models, treatment with antipsychotic drugs can induce changes in DNA methylation of neuroregulatory genes such as dopamine receptor family genes, cadherin family genes, and neurotrophic factor genes, and thus, affect their expression profiles and animal behavioral phenotypes^{14,15,16}. Antipsychotic medication reduces chronic inflammation in patients with SCZ by modifying the secretion of inflammatory cytokines and activation of peripheral immune cells^{17,18,19}.

Therefore, we aimed to determine the effect of DNA methylation changes on self-tolerance breakdown in SCZ. Goals of the present study included (1) analyzing the genome-wide DNA methylation profiles in SCZ case-control cohorts to identify immune-related DMS, (ii) measuring the autoantibody levels encoded by causal candidate genes, and (iii) analyzing the correlation between these biomarkers and the clinical psychopathology of patients with SCZ.

Material And Methods

Experimental Design

A multi-stage, case-control study and a follow up plan were designed to investigate whether differences in DNA methylation in SCZ affect autoimmune responses and correlate with clinical symptoms (Figure S1).

Sample Description

A total of 2722 Chinese Han origin subjects were recruited in this study (2005–2011), including 1390 paranoid schizophrenia patients according to ICD-10 (F20.0) and 1332 controls (Table 1). All the patients were diagnosed by two consultant psychiatrists following a structured interview assessment process. The participants met all the inclusion criteria, without any exclusion criteria (Table S1). All participants provided written informed consent, and the study was approved by the local ethics committees and conformed to the requirements of the Declaration of Helsinki.

Table 1
Demographic and clinical features of the participants.

Demographic information														
Discovery Cohort					Replication Cohort					Validation Cohort				
	Age, y	SD	Male	Female		Age, y	SD	Male	Female		Age, y	SD	Male	Female
RSCZ (n = 40)	25.08	7.04	20	20	RSCZ (n = 64)	25.48	7.67	31	33	SCZ (n = 1230)	39.58	13.61	698	532
NRSCZ (n = 40)	24.23	8.43	18	22	NRSCZ (n = 16)	21.06	4.43	5	11	CTL (n = 1208)	37.39	13.61	544	644
CTL (n = 40)	25.51	5.39	20	20	CTL (n = 84)	28.77	8.58	30	54					
PANSS scores														
Baseline	Discovery Cohort					Replication Cohort					Meta			
	RSCZ	SD	NRSCZ	SD	P value	RSCZ	SD	NRSCZ	SD	P value	RSCZ	SD	NRSCZ	SD
PANSS Positive Subscales	23.00	5.32	23.20	4.57	0.012	22.75	5.13	22.00	4.47	0.122	23.35	5.04	22.52	4.19
PANSS Negative Subscales	21.08	7.54	23.23	6.75	0.079	21.06	6.27	18.19	6.72	0.015	21.39	6.79	22.10	6.92
General Psychopathology Subscales	42.05	6.90	41.25	7.27	0.992	42.34	6.81	38.38	5.77	0.009	42.76	6.97	40.67	6.41
PANSS Total	86.03	14.04	87.68	14.60	0.382	86.23	12.34	78.56	10.15	0.001	87.46	13.07	85.29	12.47
Endpoint	Discovery Cohort					Replication Cohort					Meta			
	RSCZ	SD	NRSCZ	SD	P value	RSCZ	SD	NRSCZ	SD	P value	RSCZ	SD	NRSCZ	SD
PANSS Positive Subscales	7.15	0.48	9.70	4.40	0.501	7.16	0.51	9.44	2.73	7.30E-06	7.12	0.45	9.54	3.52
PANSS Negative Subscales	9.03	2.71	16.03	5.61	4.87E-11	8.78	1.98	14.36	4.33	1.64E-08	8.89	2.37	15.88	5.16
General Psychopathology Subscales	18.60	2.31	22.48	6.11	4.10E-04	18.08	1.79	22.38	4.01	1.07E-06	18.24	2.03	22.35	5.36
PANSS Total	34.78	4.38	48.20	13.12	4.98E-09	34.03	3.08	46.18	7.33	8.65E-13	34.25	3.66	47.77	10.78
Abbreviations:														
RSCZ, remitter of schizophrenia; NRSCZ, non-remitter of schizophrenia; CTL, control; SCZ, schizophrenia; PANSS, positive and negative syndrome scale; SD, s deviations.														

A total of 160 FES patients derived from a previous trial (ClinicalTrials, identifier NCT01057849) underwent a one year follow-up study under treatment with atypical antipsychotics, including risperidone, aripiprazole, and olanzapine (2008–2011)²⁰. The definition of remission was the simultaneous attainment of symptomatic and duration criteria according to the positive and negative syndrome scale (PANSS), as proposed by the Remission in Schizophrenia Working Group²¹.

Genome-Wide DNA Methylation Profiling

In total, 200 samples from the discovery cohort were hybridized with the Illumina Human MethylationEPIC BeadChip arrays to profile the genome-wide methylation levels at more than 850,000 CpG sites. For data quality control, any technically unreliable probes were removed, including cross-hybridizing probes, probes located on sex chromosomes and SNPs overlapping probes. Methylation levels for each site were calculated using the R minfi package (version 1.28.4) and adjusted *M* values were used to run all statistical analysis²². However, β values were used for ease of clarity and interpretation. The R sva package (version 3.30.1) was performed to correct for batch effects²³. For extraction of DMS, we fitted a linear regression model for each CpG site: *M* value + age + error, and next applied an empirical Bayes smoothing to the standard errors using the R Bioconductor limma package (version 3.38.3)²⁴. DMS were extracted using a threshold of FDR-adjusted *P* value < 0.01 and the mean β value difference $|\Delta\beta| > 5\%$. GO functional enrichment analysis of genes harboring DMS was performed using the R clusterProfiler package (v3.10.1) with a FDR-adjusted *P* value < 0.05 for statistical significance.

Sequenom MassARRAY DNA quantitative methylation assay

A Sequenom MassARRAY platform was used to perform the quantitative methylation analysis of candidate DMS. The PCR primers listed in Table S2 were designed using Sequenom Epidesigner (<http://www.epidesigner.com>). For each reverse primer, an additional T7 promoter tag for in vivo transcription was added, whereas a 10 mer tag on the forward primer was used to adjust melting temperature differences. After PCR amplification, in vitro RNA transcription was performed on the reverse strand and then digested via base-specific cleavage. Mass spectra were obtained via MassARRAY Compact MALDI-TOF (Sequenom, CA, USA) and their methylation ratios were generated using Epityper software (Sequenom, CA, USA).

Detection of BICD2 transcripts expression levels

A taqman-probe based multiplex-qRT-PCR method was used for detecting the *BICD2* transcript levels. The primers and probes listed in Table S2 were designed using Primer Express™ Software v3.0.1 (Applied Biosystems, CA, USA), and their location were marked in the Figure S2.

In brief, for total *BICD2* quantification, the primer and probe sets of *BICD2* total and *GAPDH* were added in a reaction, which occupied HEX channel and FAM channel, respectively. Similarly, *BICD2* total & *BICD2* isoform 1 (NM_001003800) and *BICD2* total & *BICD2* isoform 2 (NM_015250) combinations were used for each transcript, respectively. Amplifications were performed in a Roche LightCycler® 96 system (Roche, IN, USA), using the default cycling conditions for 45 cycles. All samples were performed in triple independently biological repeats, and the results were calculated by $2^{-(\Delta Ct_{SCZ} - \Delta Ct_{CTL})}$ formula.

Detection of plasma anti-BICD2 IgG antibody levels

The computational prediction of the HLA-II epitopes was performed in the Immune Epitope Database (25) and found a 24 amino acid linear peptide (SDRAEGTGLANQVFCSEKHSIYCD) on the C-terminal tail of BICD2 isoform 1 protein as a potential autoantigen (Figure S3).

A previously reported in-house ELISA assay was optimized for plasma anti-BICD2 IgG antibodies detection⁴. The 24mer linear epitope was synthesized by solid-phase chemistry with a purity of >95% (Bootech, Shanghai, China), and dissolved in 67% acetic acid to a concentration of 5 mg/mL and stored at -20°C. The stock solution was diluted in coating buffer (0.1 M phosphate buffer, 0.15 M NaCl, 10 mM EDTA and pH 7.2) to a concentration of 20 µg/mL as working solution. A maleimide activated ELISA plate (Corning, ME, USA) was coated with 100 µL/well of working solution and incubated 2 h at room temperature (RT). The plates were washed 3 times using 200 µL/well of wash buffer 1 (0.1 M phosphate buffer, 0.15 M NaCl and pH 7.2), and blocked using 10 µg/mL cysteine in coating buffer for 1 h at RT. Then washed twice using wash buffer 1 and dried at 60°C for 3 h. Seal the dried plates and stored at 4°C until use. The coated plates needed to be rehydrated before use by washed twice with 200 µL/well of wash buffer2 (0.01 M phosphate-buffered saline (PBS) containing 0.1% Tween-20). Plasma samples as well as positive control (PC) and quality control (QC) were diluted 1:100 in assay buffer (0.01 M PBS containing 0.5% bovine serum albumin) and loaded 50 µL/well, while 50 µL of assay buffer was added to each negative control (NC) well. All samples were performed in twice independent biological repeats. The plates were incubated at RT for 2 h and then washed 3 times with wash buffer 2.

A peroxidase-conjugated goat anti-human IgG Fc secondary antibody (ab98624, Abcam, Cambridge, UK) was diluted 1:50,000 in assay buffer loaded 100 µL/well and incubated for 2 h at 4°C and washed 3 times. Finally, loaded 100 µL/well of 3, 3', 5, 5'-tetramethylbenzidine (TMB, PR1210, Solarbio, Beijing, China) and incubated in the dark for 20 min before 50 µL/well of the stop solution (12% sulphuric acid) was added. The optical density (OD) of each well was then measured within 10 min with a plate reader at 450 nm with a reference wavelength of 620 nm. The specific binding ratio (SBR) was calculating for each sample using the following formula:

$$SBR = (OD_{\text{sample}} - OD_{\text{NC}}) / (OD_{\text{PC}} - OD_{\text{NC}})$$

Statistical Analysis

Results are presented as mean with SD unless otherwise stated. A univariate linear model was used to compare the differences of demographic, PANSS, DNA methylation, and anti-BICD2 IgG levels between groups, which considered age and gender as covariates. Paired t-test was used to compare the differences between baseline and endpoint samples. Pearson's correlation analysis was used to test the correlation in cg14341177 methylation, anti-BICD2 IgG, and PANSS scores. The coefficient of variation (CV) was used to represent an inter-assay deviation using a quality control (QC) sample, which were randomly collected from 50 healthy subjects, pooled, and tested on every 96-well microtiter plate. A *P* value < 0.05 was considered to be statistically significant in this study. Analyses were performed on the IBM SPSS Statistics software (Version 20.0., IBM Corp., Armonk, NY, USA) or GraphPad software (Version 6.01, San Diego, CA, USA).

Results

Demographic and clinical characteristics of the subjects

In the 160 SCZ patients who completed the 1-year of antipsychotic treatment, there was no difference between remitters of schizophrenia (RSCZ) and non-remitters of schizophrenia (NRSCZ) in terms of baseline demographic and clinical characteristics. At the endpoint of 1-year follow-up, 56 NRSCZ showed higher PANSS scores than RSCZ (Table 1). The remaining 1230 SCZ patients were diagnosed in acute schizophrenic episode. All control subjects (CTL) have no mental illness or family history.

We thus divided these subjects into a discovery cohort, a replication cohort and a validation cohort. The discovery cohort contained 40 RSCZ, 40 NRSCZ and 40 CTL subjects well matched in age and sex. The replication cohort contained the remaining 64 RSCZ and 16 NRSCZ, as well as 84 CTL subjects. The enlarged cross-sectional validation cohort contained 1230 SCZ and 1208 CTL subjects (Table 1).

Genomic differences in DNA methylation profiles in RSCZ and NRSCZ

We firstly analyzed the genome-wide DNA methylation variation at > 850,000 CpG sites in the discovery cohort. After normalization and filtering of data, we retained a final dataset of 682,651 CpG sites in the 120 subjects. Principal component (PC) analysis showed a clear distinction between RSCZ and NRSCZ from CTL along the first two PCs (Fig. 1A). However, the difference was less between baseline and endpoint DNA samples, indicating that the antipsychotic medications did not cause global DNA methylation changes. A total of 53,659 DMS were identified and mapped to 11,749 genes at a 1% FDR and a mean difference ($\Delta \beta$) > 5% (Table S3).

The genomic distribution of DMS was quite different between RSCZ and NRSCZ groups. In RSCZ, hyper-methylated DMS were enriched in 5'-UTR, gene body, 3'-UTR and enhancer region, while hypo-methylated DMS were enriched in TSS200, 5'-UTR, 1st exon and promoter. In NRSCZ, hyper-methylated DMS were enriched in TSS200, 5'-UTR, 1st exon and enhancer, but no hypo-methylated DMS enriched region was found (Fig. 1B). There were more state-dependent DMS in the RSCZ group (476 DMS) than the NRSCZ group (17 DMS) when comparing their baseline and endpoint samples (Table S4-5). The cg14341177 was the foremost hyper-methylated DMS in the baseline DNA samples of the RSCZ group (fold change [FC] = 4.171, P = 1.42E-11), and its level decreased in the endpoint DNA samples (FC = -3.397, P = 2.41E-7). A similar state-dependent change was observed in case of the foremost hypo-methylated DMS cg13978347 (Baseline: FC = -2.666, P = 1.59E-6; Endpoint: FC = 2.325, P = 3.02E-4). However, these changes were not found in the NRSCZ group (Fig. 1C, Table S4-5). Gene Ontology (GO) analysis of genes corresponding to DMS also showed different clustered biological processes between the RSCZ and NRSCZ. The top 10 enriched pathways in the RSCZ group were mostly associated with the regulation of T cells and neutrophils; however, those in the NRSCZ group were associated with extracellular matrix, neuronal guidance and synaptic signal transmission (Fig. 1D, Table S6).

Validation of candidate DMS by quantitative methylation assay

A Sequenom MassARRAY quantitative methylation assay was performed to measure the methylation levels of candidate DMS cg14341177 and cg13978347 in the discovery cohort. There are 4 CpG sites on cg14341177, in which the CpG2 site showed the most significant changes in methylation levels and seemed as the leading CpG site. In the baseline DNA samples, the methylation level of CpG2 was higher in the RSCZ (FC = 1.40, P = 8.338E-11) and NRSCZ group (FC = 1.12, P = 0.027) than those in the CTL group. In the endpoint DNA samples, the methylation level of CpG2 was significantly lower in the RSCZ group (FC = 0.80, P = 3.329E-7) than those in the baseline samples, but not in the NRSCZ group (FC = 1.03, P = 0.210) (Table 2). However, significant changes in the DNA methylation levels of cg13978347 were not observed, and therefore, were not considered for further analysis (Table 2). We got similar results in the replication cohort of 164 independent subjects (64 RSCZ, 16 NRSCZ, and 80 CTL), the hyper-methylation levels of cg14341177 were state-dependent in RSCZ (Baseline: FC = 1.15, P = 3.577E-6; Endpoint: FC = 0.83, P = 3.48E-7) but not in NRSCZ (Table 2). These results were further confirmed in the validation cohort (1230 SCZ vs. 1208 CTL) and were finely reproduced (FC = 1.26, P = 1.896E-145) (Fig. 2).

Table 2
Quantitative methylation assay for candidate DMS.

Position	CTL	RSCZ				NRSCZ				RSCZ				NRS
		SD	Baseline	SD	Endpoint	SD	Baseline	SD	Endpoint	SD	Baseline v.s. CTL ^a	Endpoint v.s. CTL ^a	Baseline v.s. End-Point ^b	
Discovery Cohort														
cg14341177														
CpG_1	0.823	0.040	0.855	0.019	0.843	0.030	0.833	0.026	0.838	0.022	4.98E-05	0.033	0.025	0.29
CpG_2	0.200	0.045	0.280	0.045	0.225	0.040	0.223	0.047	0.231	0.047	8.34E-11	0.009	3.33E-07	0.02
CpG_3&4	0.830	0.033	0.840	0.050	0.825	0.068	0.834	0.028	0.844	0.032	0.361	0.723	0.324	0.61
DMS	0.618	0.029	0.656	0.030	0.631	0.034	0.630	0.027	0.638	0.030	1.69E-07	0.084	3.51E-04	0.08
cg13978347														
CpG_1	0.735	0.087	0.744	0.056	0.735	0.083	0.730	0.070	0.749	0.112	0.599	0.627	0.986	0.70
CpG_2	0.868	0.175	0.851	0.181	0.882	0.141	0.873	0.114	0.867	0.136	0.357	0.753	0.458	0.48
CpG_3	0.978	0.039	0.996	0.039	0.971	0.071	0.970	0.057	0.975	0.064	0.452	0.562	0.388	0.26
DMS	0.860	0.076	0.856	0.072	0.863	0.063	0.857	0.048	0.861	0.050	0.663	0.839	0.748	0.33
Replication Cohort														
cg14341177														
CpG_1	0.833	0.019	0.833	0.024	0.831	0.019	0.827	0.023	0.823	0.019	0.993	0.921	0.559	0.07
CpG_2	0.202	0.026	0.233	0.043	0.193	0.035	0.206	0.038	0.209	0.046	3.58E-06	0.376	3.48E-07	0.25
CpG_3&4	0.832	0.033	0.830	0.038	0.834	0.029	0.838	0.029	0.833	0.024	0.499	0.784	0.506	0.14
DMS	0.622	0.018	0.631	0.026	0.620	0.019	0.622	0.024	0.624	0.022	0.062	0.635	0.003	0.00
Abbreviations: CTL, control; RSCZ, remitter of schizophrenia; NRSCZ, non-remitter of schizophrenia, DMS, differential methylation site. Superscripts: a. <i>P</i> value model; b. paired t-test <i>P</i> values.														

Hyper-methylation of cg14341177 may inhibit alternative-splicing of BICD2 mRNA in patients with SCZ

The DMS cg14341177 is located on exon 7 of the bicaudal D cargo adaptor 2 (*BICD2*) gene and next to the 3'-end of the alternative splicing region in *BICD2* isoform 1 mRNA (alternative intron 7, I7'), the splicing of which leads to a truncated *BICD2* isoform 2 (Figure S2). A higher level of I7' has been reported in the blood and mortem brain samples in SCZ²⁵. We thus speculated that the hyper-methylation in the DMS cg14341177 may affect the alternative splicing events of *BICD2*. We detected *BICD2* mRNA levels in the peripheral blood mononuclear cells (PBMCs) of 155 subjects (59 CTL vs. 96 SCZ) by performing isoform-specific qRT-PCR. No significant changes were found in the levels of total *BICD2* and *BICD2* isoform 2 mRNAs. However, *BICD2* isoform 1 mRNA levels were significantly higher in patients with SCZ (FC = 2.4, $P < 0.0001$) (Fig. 3A). A significantly positive correlation was observed between *BICD2* isoform 1 mRNA and cg14341177 methylation levels ($r = 0.4717$, $P < 0.0001$), whereas a significant negative correlation was observed between *BICD2* isoform 2 mRNA and cg14341177 methylation levels ($r = -0.1867$, $P = 0.0349$), respectively (Fig. 3B). These results suggested that the hyper-methylation in the DMS cg14341177 could inhibit the alternative splicing of *BICD2* mRNAs.

Plasma BICD2 IgG antibody levels increased in patients with SCZ

According to the data obtained from Human Protein Atlas database, BICD2 is widely expressed in the brain and peripheral immune cells, especially in the cortex, hippocampus, amygdala, B lymphocytes, neutrophils, and dendritic cells (Figure S4)²⁶. This implies that BICD2 may have some role in the neuroimmunity process. The BICD2 isoform 1 protein has an extra C terminal tail of 31 amino acid residues, which comprises a 24-mer linear autoantigen predicted by IEDB (Figure S3A)^{27,28}. We thus speculated that the inhibition of *BICD2* mRNA splicing by hyper-methylation in the DMS cg14341177 may affect the levels of circulating anti-BICD2 IgG autoantibodies. By performing an in-house ELISA assay against the autoantigen of BICD2 (Figure S3B), plasma anti-BICD2 IgG levels of 1011 subjects (486 CTL vs. 525 SCZ) were measured and significantly elevated anti-BICD2 IgG was detected in SCZ samples (FC = 1.68, $P < 0.0001$) (Fig. 4A). The reproducibility of the ELISA assay was excellent, with an inter-assay coefficient of variation of 9.3% for a total of 31 plates. In the follow-up cohorts, anti-BICD2 IgG levels decreased in the RSCZ endpoint samples (FC = 0.78, $P < 0.0001$), whereas the levels slightly increased in the NRSCZ samples (FC = 1.07, $P = 0.0136$) (Fig. 4B).

Correlation between cg14341177 DNA methylation, anti-BICD2 IgG, and PANSS scores

The above results showed that the levels of cg14341177 methylation and anti-BICD2 IgG levels can be considered as potential biomarkers for SCZ and its state of remission. Pearson's correlation analysis was performed for all the patients in the follow-up cohorts. In the RSCZ group, a strong positive correlation was observed between cg14341177 methylation and anti-BICD2 IgG levels in the baseline ($r = 0.2762$, $P = 0.0045$), and was most significant in the leading CpG2 ($r = 0.4732$, $P < 0.0001$). A similar correlation was observed when CpG2 and anti-BICD2 IgG levels were compared with PANSS negative subscale scores (CpG2: $r = 0.5052$, $P < 0.0001$; anti-BICD2 IgG: $r = 0.05969$, $P < 0.0001$) and PANSS total scores (CpG2: $r = 0.3242$, $P = 0.0008$; anti-BICD2 IgG: $r = 0.3731$, $P < 0.0001$), respectively. However, a non-significant correlation was observed in the NRSCZ group (Fig. 5 and Table S7).

Discussion

The present study confirmed that extensive differences exist in global DNA methylation profiles between first-episode RSCZ and NRSCZ, as well as the genomic distribution of DMS, and DMS harbored genes and their biological processes. The DMS cg14341177 was the foremost hyper-methylated DMS with decreased methylation levels in the RSCZ group after the administration of antipsychotic medications for one year, but not in the NRSCZ group. Moreover, the hyper-methylated cg14341177 may inhibit the alternative splicing of its harbored gene *BICD2*, resulting in the increase of its longer isoform 1 transcript products. The plasma anti-BICD2 IgG levels were also increased in SCZ, and their change patterns were similar to cg14341177 methylation in the follow-up cohorts. Lastly, the alterations in cg14341177 methylation, plasma anti-BICD2 IgG, and PANSS negative subscale scores were highly correlated in the RSCZ group, and not in the NRSCZ group.

BICD2 gene is located on 9q22.31, and encodes a conserved cargo adaptor protein required for dynein-mediated transportation. Functionally, BICD2 has been reported to be localized in the Golgi complex and participates in membrane traffic from the Golgi apparatus toward the endoplasmic reticulum (ER) via a coat complex coatamer protein I (COPI)-independent pathway²⁹. In mice, the deficiency of *BICD2* affects radial cerebellar migration of granule cells in the developing brain³⁰. In humans, coding mutations were also found in spinal muscular atrophy^{31,32}. In PBMCs, *BICD2* is most abundant in naive B lymphocytes (Figure S4). A recent study confirmed that a dynein subunit (DYNLL1) is particularly critical for the development of B-1a lymphocytes, which is a major source of autoantibodies and natural antibodies³³. Thus the increase of anti-BICD2 IgG levels may disrupt the dynein-mediated cargo transportation in neurons and B lymphocytes, and further breakdown the neuro-immune crosstalk in SCZ. Further investigations are wanted to explore the underlying mechanism by which BICD2 may play a central role in regulating dynein-mediated transport in neuro-immune processes.

Hyperactivity of immune components contributes to the etiology of SCZ to some extent. Previous studies have suggested that increased levels of pro-inflammatory molecules in both acute and chronic SCZ, as well as antipsychotic medications can reduce inflammation in some patients with SCZ^{34,35}. Antipsychotic medications can also reduce disease severity, inflammatory cytokines, and autoantibody levels in autoimmune encephalomyelitis, which has overlapped clinical symptoms with SCZ³⁶. This is probably because of the wide distribution of dopaminergic and serotonergic receptors in immune cells, antipsychotic drugs treatment could regulate the differentiation and maturation of immune cells and further their responses^{37,38}. We thus speculated that some common regulatory mechanisms may be involved in brain and peripheral lymphocytes in patients with SCZ, and especially those involving autoreactive processes. However, the underlying neuro-immune regulatory mechanisms may vary and more efforts are required.

This study has some limitations. First, the confounding effects of lifestyle-related factors such as smoking, alcohol consumption, and diet in patients were not controlled in this study. Second, the validation cohort subjects were a mix of first-onset and chronic patients with SCZ, as well as drug-free and medication patients. These factors may have interfered with the assay results to some extent. Third, limited clinical information of the subjects was available such as history of autoimmune disorders or hypersensitivities that may have affected our analysis, although the prevalence of autoimmune conditions is no more than 2% in the Chinese population³⁹. It would also be useful to test these biomarkers in individuals with bipolar or autism spectrum disorders, or other psychiatric diseases to determine if these abnormalities are limited to SCZ.

Declarations

Acknowledgements

This work was supported by the research grants from the National Natural Science Foundation of China (82071504, 81625008, 81930104), the National Key Research and Development Program of China (2016YFC1307004), Beijing Municipal Science & Technology Commission (Z181100001518001, D171100007017002), CAMS Innovation Fund for Medical Sciences (2016-I2M-1-004).

Author contributions

Q.X and X.Y conceived the project. H.W, Y.Y, C.Z contributed equally to this work. All authors contributed to the experimental design, analysis, and interpretation of results. Study concept and design: H.W, X.Y, Q.X. Acquisition of data: All authors. Clinical data and biological sample collection: Y.Y, F.Y, Z.L, C.W, H.D, J.Z, R.T. Drafting of the manuscript: H.W, X.Y, Q.X. Statistical analysis: H.W, C.Z. Obtained funding: H.W, X.Y, Q.X. Study supervision: H.W, X.Y, Q.X. All authors have reviewed and approved the final paper.

CONFLICT OF INTEREST

The authors report no financial interests or potential conflicts of interest.

Additional information

Supplementary information

Supplementary Data are available at *Nature Communications* online.

Correspondence and requests for materials should be addressed to Q.X or X.Y.

References

1. Saraceno B. The WHO World Health Report 2001 on mental health. *Epidemiologia e psichiatria sociale* **11**, 83–87 (2002).
2. Schizophrenia Working Group of the Psychiatric Genomics C. Biological insights from 108 schizophrenia-associated genetic loci. *Nature* **511**, 421–427 (2014).
3. Cross-Disorder Group of the Psychiatric Genomics Consortium. Electronic address pmhe, Cross-Disorder Group of the Psychiatric Genomics C. Genomic Relationships, Novel Loci, and Pleiotropic Mechanisms across Eight Psychiatric Disorders. *Cell* **179**, 1469–1482 e1411 (2019).
4. Whelan R, St Clair D, Mustard CJ, Hallford P, Wei J. Study of Novel Autoantibodies in Schizophrenia. *Schizophr Bull*, (2018).
5. Li C, *et al.* Anti-TSNARE1 IgG plasma levels differ by sex in patients with schizophrenia in a Chinese population. *FEBS open bio* **9**, 1705–1712 (2019).
6. Maric NP, Svrakic DM. Why schizophrenia genetics needs epigenetics: a review. *Psychiatria Danubina* **24**, 2–18 (2012).
7. Swathy B, Banerjee M. Understanding epigenetics of schizophrenia in the backdrop of its antipsychotic drug therapy. *Epigenomics* **9**, 721–736 (2017).
8. Mendizabal I, *et al.* Cell type-specific epigenetic links to schizophrenia risk in the brain. *Genome biology* **20**, 135 (2019).
9. Melas PA, Rogdaki M, Osby U, Schalling M, Lavebratt C, Ekstrom TJ. Epigenetic aberrations in leukocytes of patients with schizophrenia: association of global DNA methylation with antipsychotic drug treatment and disease onset. *FASEB journal: official publication of the Federation of American Societies for Experimental Biology* **26**, 2712–2718 (2012).
10. Montano C, *et al.* Association of DNA Methylation Differences With Schizophrenia in an Epigenome-Wide Association Study. *JAMA psychiatry* **73**, 506–514 (2016).
11. Wockner LF, *et al.* Genome-wide DNA methylation analysis of human brain tissue from schizophrenia patients. *Translational psychiatry* **4**, e339 (2014).
12. Zhao Y, *et al.* A large-scale integrative analysis of GWAS and common meQTLs across whole life course identifies genes, pathways and tissue/cell types for three major psychiatric disorders. *Neuroscience and biobehavioral reviews* **95**, 347–352 (2018).
13. Pries LK, Guloksuz S, Kenis G. DNA Methylation in Schizophrenia. *Advances in experimental medicine and biology* **978**, 211–236 (2017).
14. Melka MG, Castellani CA, Laufer BI, Rajakumar RN, O'Reilly R, Singh SM. Olanzapine induced DNA methylation changes support the dopamine hypothesis of psychosis. *Journal of molecular psychiatry* **1**, 19 (2013).
15. Melka MG, Castellani CA, Rajakumar N, O'Reilly R, Singh SM. Olanzapine-induced methylation alters cadherin gene families and associated pathways implicated in psychosis. *BMC neuroscience* **15**, 112 (2014).
16. Dong E, Tueting P, Matrisciano F, Grayson DR, Guidotti A. Behavioral and molecular neuroepigenetic alterations in prenatally stressed mice: relevance for the study of chromatin remodeling properties of antipsychotic drugs. *Translational psychiatry* **6**, e711 (2016).
17. Azizi E, Zavaran Hosseini A, Soudi S, Noorbala AA. Alteration of Serum Levels of Cytokines in Schizophrenic Patients before and after Treatment with Risperidone. *Iranian journal of allergy, asthma, and immunology* **18**, 262–268 (2019).
18. Chen ML, *et al.* Antipsychotic drugs suppress the AKT/NF-kappaB pathway and regulate the differentiation of T-cell subsets. *Immunology letters* **140**, 81–91 (2011).
19. Chen ML, Wu S, Tsai TC, Wang LK, Tsai FM. Regulation of macrophage immune responses by antipsychotic drugs. *Immunopharmacology and immunotoxicology* **35**, 573–580 (2013).
20. Cheng Z, *et al.* Which Subgroup of First-Episode Schizophrenia Patients Can Remit During the First Year of Antipsychotic Treatment? *Frontiers in psychiatry* **11**, 566 (2020).
21. Andreasen NC, Carpenter WT, Jr., Kane JM, Lasser RA, Marder SR, Weinberger DR. Remission in schizophrenia: proposed criteria and rationale for consensus. *The American journal of psychiatry* **162**, 441–449 (2005).
22. Aryee MJ, *et al.* Minfi: a flexible and comprehensive Bioconductor package for the analysis of Infinium DNA methylation microarrays. **30**, 1363–1369 (2014).
23. Leek JT, Johnson WE, Parker HS, Jaffe AE, Storey JDJB. The sva package for removing batch effects and other unwanted variation in high-throughput experiments. **28**, 882–883 (2012).
24. GK S. Limma: linear models for microarray data. In: *Bioinformatics and computational biology solutions using R and Bioconductor* (ed Gentleman R CV, Dudoit S, Irizarry I, Hube W). Springer (2005).
25. Oldmeadow C, *et al.* Combined analysis of exon splicing and genome wide polymorphism data predict schizophrenia risk loci. *Journal of psychiatric research* **52**, 44–49 (2014).
26. Uhlen M, *et al.* Proteomics. Tissue-based map of the human proteome. *Science* **347**, 1260419 (2015).
27. Vita R, *et al.* The Immune Epitope Database (IEDB): 2018 update. *Nucleic acids research* **47**, D339–D343 (2019).
28. UniProt C. UniProt: a worldwide hub of protein knowledge. *Nucleic acids research* **47**, D506–D515 (2019).
29. Matanis T, *et al.* Bicaudal-D regulates COPI-independent Golgi-ER transport by recruiting the dynein-dynactin motor complex. *Nature cell biology* **4**, 986–992 (2002).

30. Jaarsma D, *et al.* A role for Bicaudal-D2 in radial cerebellar granule cell migration. *Nature communications* **5**, 3411 (2014).
31. Rossor AM, *et al.* Phenotypic and molecular insights into spinal muscular atrophy due to mutations in BICD2. *Brain: a journal of neurology* **138**, 293–310 (2015).
32. Peeters K, *et al.* Molecular defects in the motor adaptor BICD2 cause proximal spinal muscular atrophy with autosomal-dominant inheritance. *American journal of human genetics* **92**, 955–964 (2013).
33. King A, *et al.* Dynein light chain regulates adaptive and innate B cell development by distinctive genetic mechanisms. *PLoS genetics* **13**, e1007010 (2017).
34. Khandaker GM, Cousins L, Deakin J, Lennox BR, Yolken R, Jones PB. Inflammation and immunity in schizophrenia: implications for pathophysiology and treatment. *The Lancet Psychiatry* **2**, 258–270 (2015).
35. Muller N. Inflammation in Schizophrenia: Pathogenetic Aspects and Therapeutic Considerations. *Schizophr Bull* **44**, 973–982 (2018).
36. O'Sullivan D, *et al.* Treatment with the antipsychotic agent, risperidone, reduces disease severity in experimental autoimmune encephalomyelitis. *PLoS one* **9**, e104430 (2014).
37. McKenna F, *et al.* Dopamine receptor expression on human T- and B-lymphocytes, monocytes, neutrophils, eosinophils and NK cells: a flow cytometric study. *Journal of neuroimmunology* **132**, 34–40 (2002).
38. Levite M. Dopamine and T cells: dopamine receptors and potent effects on T cells, dopamine production in T cells, and abnormalities in the dopaminergic system in T cells in autoimmune, neurological and psychiatric diseases. *Acta physiologica* **216**, 42–89 (2016).
39. Li R, Sun X, Liu X, Yang Y, Li Z. Autoimmune diseases in China. *Advances in immunology* **144**, 173–216 (2019).

Figures

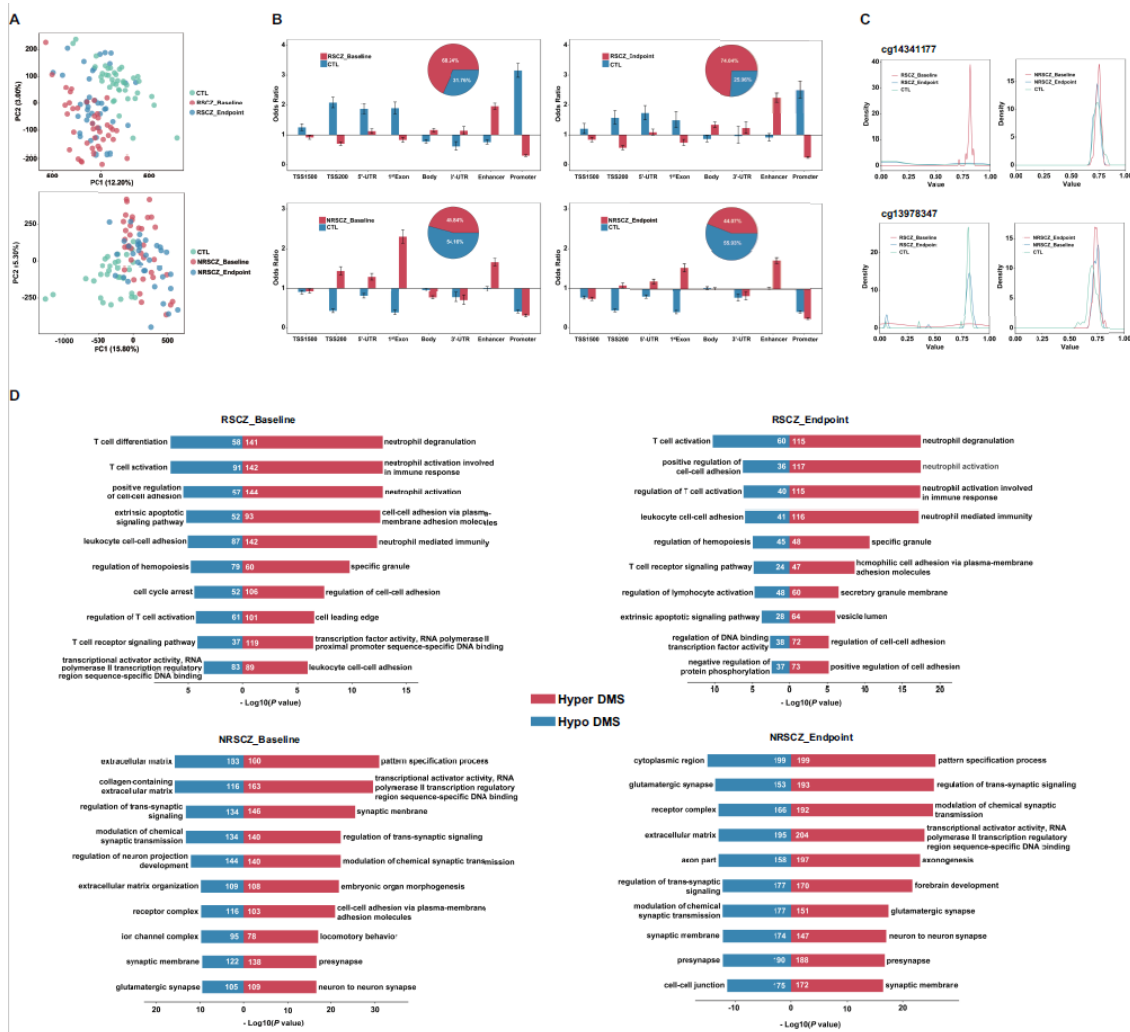


Figure 1

Group differences in DNA methylation profiles. (A) Principal component analysis (PCA) of DNA methylation profiles for all 120 individuals. Green, red and blue circles represent health control, baseline schizophrenia and endpoint schizophrenia, respectively. The proportions of variance explained by PC1 and PC2 are indicated. (B) Genomic location of differentially methylated sites (DMS), for CpG sites hyper-methylated in SCZ patients (red) and in controls (blue). Odds ratio and 95% confidence intervals are displayed, comparing their localization in different genomic locations as provided by Illumina and ChromHMM phase 15

(TSS1500, TSS200, 5'-UTR, 1st Exon, Body, 3'-UTR, Enhancer and promoter. Odds ratios were computed against the general distribution of the total detected CpGs of our dataset. Proportion of DMS those are hyper-methylated either in SCZ (red) or in CTL (blue) individuals. (C) Illustration of the foremost hyper-methylated DMS and hypo-methylated DMS in SCZ. The density of β values of CpG sites by category is given as illustrations of the group differences, with red, blue and green lines representing the methylation density in baseline schizophrenia, endpoint schizophrenia and control, respectively. (D) Gene Ontology (GO) enrichment analyses. For both groups, the top 10 GO categories reaching 5% FDR are shown, together with the number of genes per category and the \log_{10} -transformed FDR-adjusted enrichment P values.

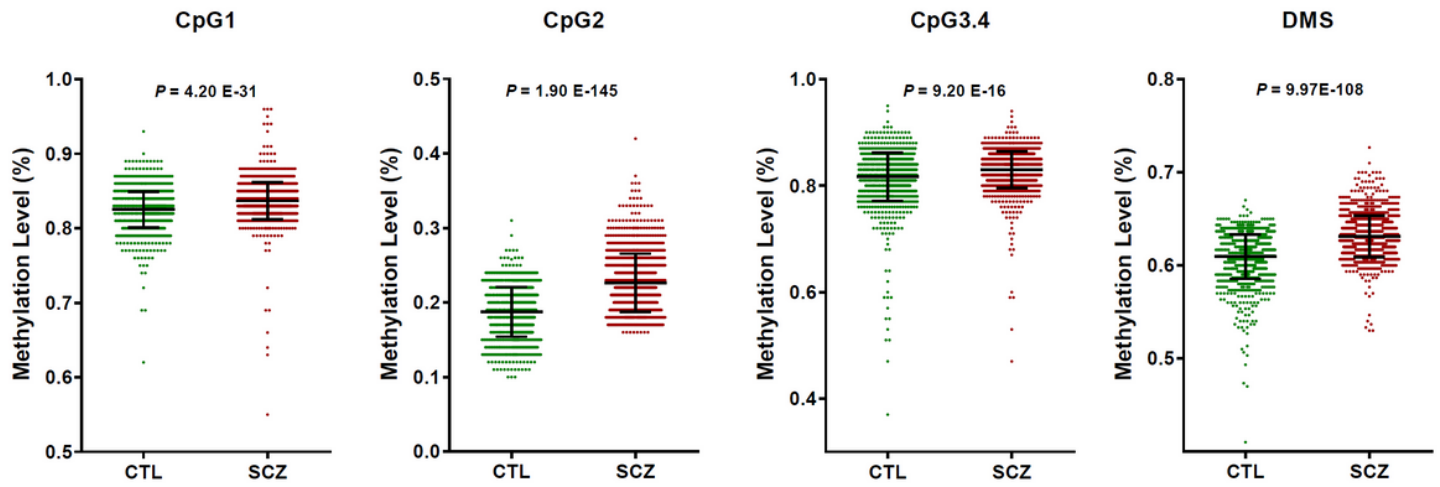


Figure 2
Quantitative methylation assay of cg14341177 in validation cohort. CTL, control; SCZ, schizophrenia; DMS, differential methylation site. Each dot represents one donor.

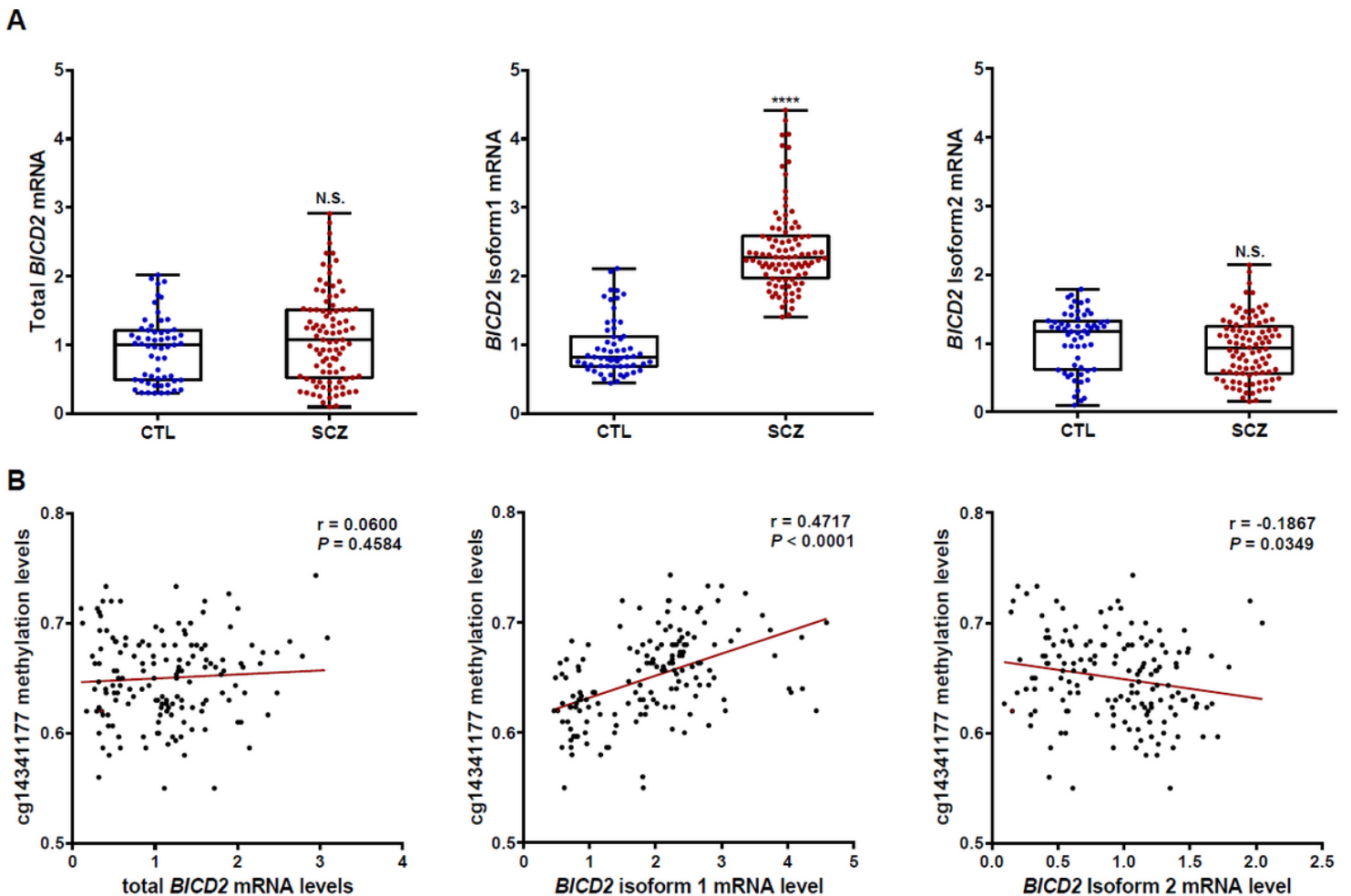


Figure 3
Page 10/12

Hyper-methylation of cg14341177 may inhibit Exon7 alternative splicing of BICD2 mRNA. (A) Quantification of BICD2 transcripts by Taqman-probe qRT-PCR in 59 CTL and 96 SCZ (normalized to GAPDH for total BICD2 or to total BICD2 for BICD2 isoform 1 and BICD2 isoform 2). (B) Pearson correlation analysis between the level of cg14341177 methylation and the level of BICD2 transcripts. Box, 1st quartile, 3rd quartile and median; each dot represents one donor; NS, not significant, **** $P < 0.0001$.

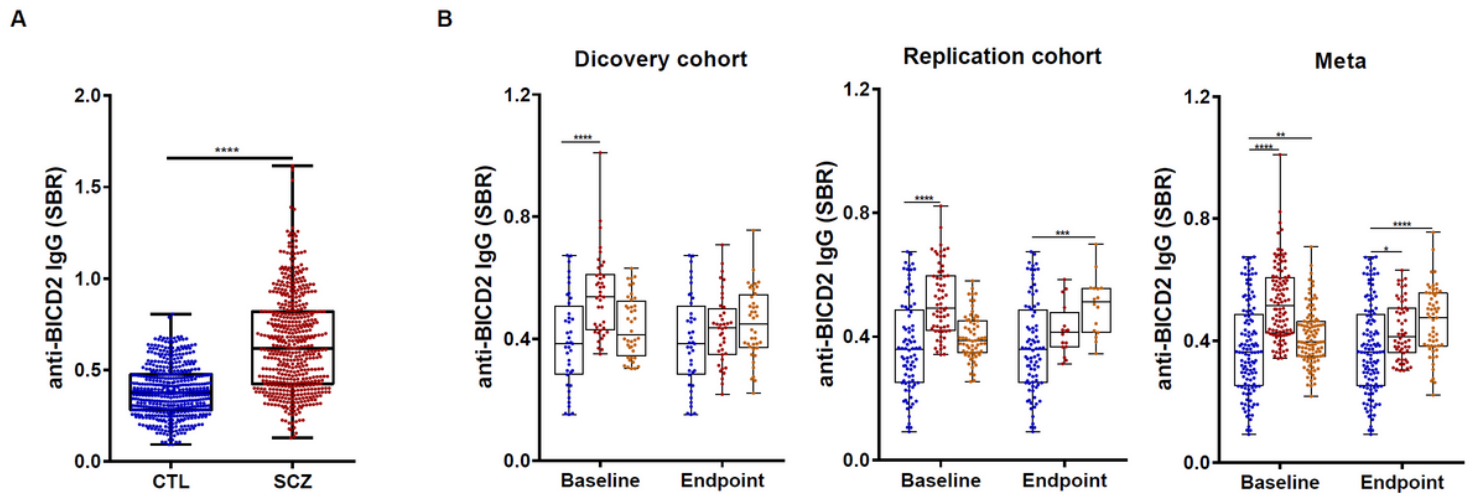


Figure 4

Upregulation of plasma anti-BICD2 IgG levels in schizophrenia. (A) Quantification of anti-BICD2 IgG levels in all available plasma samples (486 CTL v.s. 525 SCZ). (B) Comparison of the anti-BICD2 IgG changes in the discovery cohort (40 CTL, 40 RSCZ and 40 NRSCZ) and the replication cohort (84 CTL, 64 RSCZ and 16 NRSCZ). Box, 1st quartile, 3rd quartile and median; each dot represents one donor; * $P < 0.05$, ** $P < 0.01$, *** $P < 0.001$, **** $P < 0.0001$.

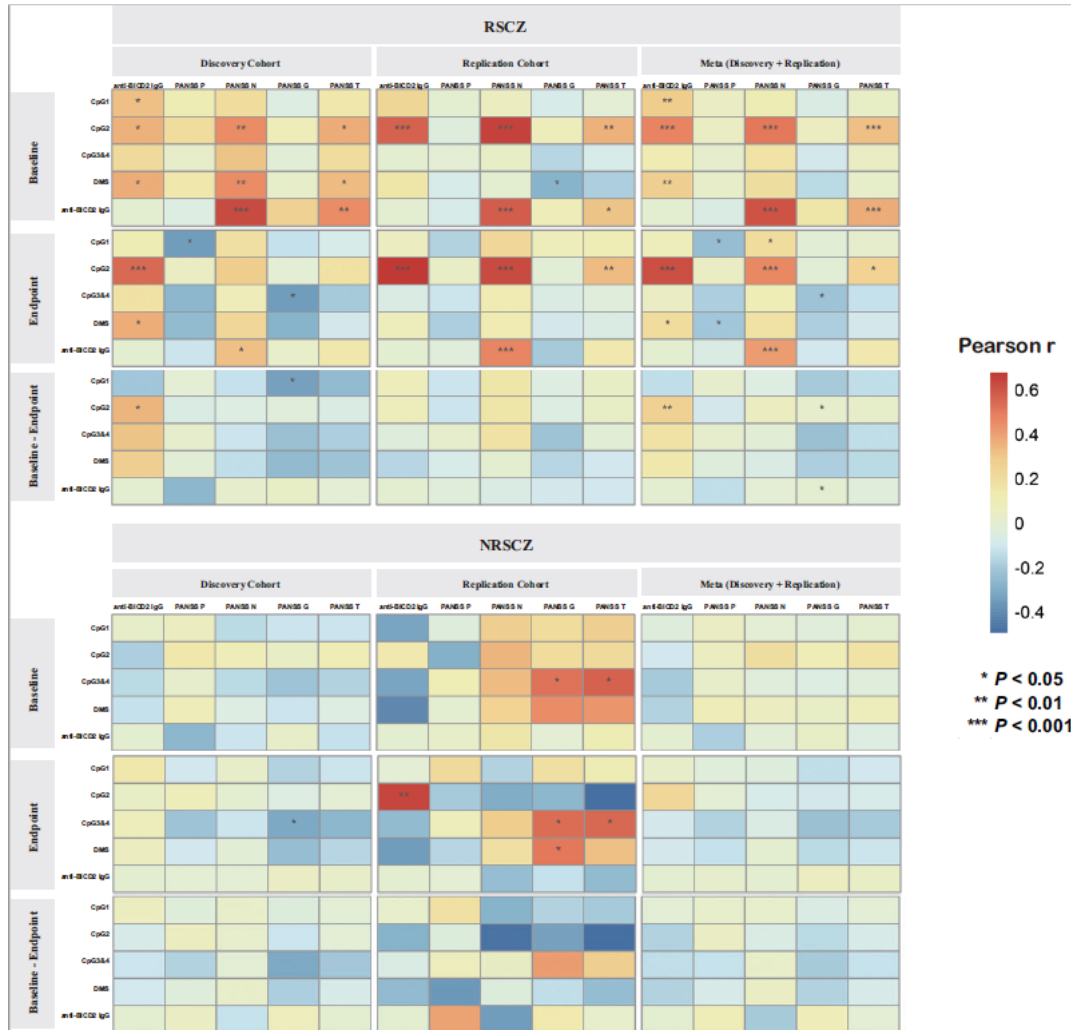


Figure 5

Correlation matrix of cg14341177 methylation, anti-BICD2 IgG and PANSS criteria scores. The darker the color, the larger the magnitude of pearson r. * P < 0.05, ** P < 0.01, *** P < 0.001.

Supplementary Files

This is a list of supplementary files associated with this preprint. Click to download.

- [Supplement2.xlsx](#)
- [Supplement1.docx](#)